1. Ahmad BOUSSOUFA[1], 2. Aimad AHRICHE[1], 3. Madjid KIDOUCHE[1], 4.Mohammed Zinelabidine DOGHMANE[1,2]

University of M'hamed Bougara of Boumerdes, Independence Avenue , 35000 Boumerdès – Algeria (1), Exploration Division, Sonatrach (2)

doi:10.15199/48.2024.02.20

Discretization Order Influences on Extended Kalman Filter Estimation for Doubly-Fed Induction Generator

***Abstract**. The main objective of this paper is to analyze the influence of the discretization step on the estimated states of the Doubly-Fed Induction Generator (DFIG). Although the Extended Kalman Filter (EKF) has been widely used for such systems, the discretization process is conventionally ensured by the first-order Forward Euler method. Therefore, the effects of the discretization order of the discrete state-space representation on the Extended Kalman Filter estimation have not been studied before. In this paper, we combine the Extended Kalman Filter with two second-order discretization methods: Central Difference and Adams-Bashforth methods, to estimate the states of a Doubly-Fed Induction Generator and improve the estimation precision of the rotor speed and the Flux of the generator. A comparative study has been conducted to analyze the qualitative and quantitative responses of the estimator for different cases. The obtained results have demonstrated the significance of the discretization order on the estimation process of the two states of the DFIG.*

***Streszczenie.** Głównym celem tej pracy jest analiza wpływu kroku dyskretyzacji na oszacowane stany Dwubiegowego Generatora Indukcyjnego (DFIG). Chociaż Rozszerzony Filtr Kalmana (EKF) jest szeroko stosowany w tego typu systemach, proces dyskretyzacji jest zazwyczaj zapewniany przez metodę pierwszego rzędu Forward Euler. Dlatego też wpływ rzędu dyskretyzacji na oszacowanie za pomocą Rozszerzonego Filtru Kalmana nie był wcześniej badany. W niniejszej pracy łączymy Rozszerzony Filtr Kalmana z dwiema metodami dyskretyzacji drugiego rzędu: różnicą centralną i metodą Adamsa-Bashfortha, aby oszacować stany Dwubiegowego Generatora Indukcyjnego oraz poprawić precyzję oszacowania prędkości wirnika i strumienia generatora. Przeprowadzono badanie porównawcze w celu analizy odpowiedzi jakościowych i ilościowych estymatora dla różnych przypadków. Uzyskane wyniki wykazały znaczenie rzędu dyskretyzacji w procesie oszacowania dwóch stanów DFIG. (**Wpływ kolejności dyskretyzacji na rozszerzoną estymację filtra Kalmana dla generatora indukcyjnego z podwójnym zasilaniem**)*

Keywords: Discretization, Doubly-Fed Induction Generator (DFIG), Extended Kalman Filter (EKF), Second-Order Method.
Słowa kluczowe: Dyskretyzacja, Dwubiegowy Generator Indukcyjny (DFIG), Rozszerzony Filtr Kalmana (EKF), Metody drugiego rzędu,

I. Introduction

State estimation is a very broad subject, as it is involved in many research areas such as control, system identification, and telecommunications, among others. It consists of inferring the states of a system based on the information provided by the process model and the taken measurements. In general, the model is not an exact replica of the behavior of the process, but it provides a good approximation with a certain level of accuracy, while the measurements are affected by noises that can reduce their accuracy. To address these imperfections, various estimation techniques have been developed, such as Maximum Likelihood Estimator (MLE) and Kalman Filter (KF).

The Kalman Filter (KF) is widely used in state estimation problems for linear dynamical systems and is known to be one of the most optimal estimators under predefined conditions. Some applications of using the KF for estimation are presented in [1–3]. However, most industrial systems exhibit nonlinear dynamic behavior, which can render the standard Kalman filter less effective. To address this limitation, modifications have been introduced to improve the accuracy of the Kalman filter for nonlinear systems, leading to the development of new algorithms such as the Extended Kalman Filter (EKF) and the Unscented Kalman Filter (UKF) [4]. The EKF is based on the linearization of the nonlinear model at each iteration around an operating point. It is widely used due to its simplicity and ease of implementation. However, in strongly nonlinear systems, the EKF often provides poor estimation results. On the other hand, the UKF is known to have better accuracy than the EKF for nonlinear systems, but it is more complex and requires more computational time. Researchers have made attempts to improve the EKF, as demonstrated in the work presented in [5], where three modified EKF algorithms have been compared in terms of their performances. These methods involve changing the integration step length using the Gauss-Newton method with Quasi-Newton technique and the Levenberg-Marquardt method. The latter introduces a damping factor to the Gauss-Newton method. Another strategy proposed in the literature involves approximating the nonlinear functions of the model using Taylor series up to the second derivative [6-7]. However, the use of second derivatives results in the computation of the Hessian matrix, making the EKF more complex and less efficient in terms of required computational time. To address this issue, Michael Roth and Frederick Gustafsson proposed a new contribution in [8] to enhance the required computational time and reduce complexity. Another modification to tackle the problem of calculating the Hessian matrix is presented in [9], wherein the algorithm used is called the Second Order Extended Particle Filter, where the EKF is used to obtain an approximation of the posterior probability density needed in the particle filter algorithm. Additional modifications to improve the accuracy of the EKF are presented in [10–13]. Another algorithm known as the "Cubature Kalman Filter" (CKF) was developed by Lenkaran Arasaratnam and Simon Haykin in 2009 [14]. This algorithm is quite similar to UKF, but it differs in the set of rules used to calculate the Kalman filter weights. The CKF uses a spherical radial cubature rule to generate the weights instead of the Sigma-points set. The CKF was designed to tackle the problems of divergence in high-dimensional nonlinear systems.

In this paper, we make an attempt to improve the accuracy of the Kalman filter for nonlinear systems without increasing the algorithm's complexity or computational inefficiency. Specifically, we propose the investigation of two second-order discretization methods (central difference and Adams-Bashforth) for the continuous nonlinear system, resulting in a second-order Extended Kalman Filter (EKF) that does not require the computation of the Hessian matrix.

The rest of the manuscript is organized as follows: in section two, the central difference and Adams-Bashforth discretization methods are carefully overviewed. In section three, the DFIG nonlinear state equations are derived in the synchronous reference frame (dq) to be used for EKF estimation. Then, in section four, the EKF combined with the different discretization methods is designed for the DFIG model. In section five, an analytical comparison is conducted for the different obtained results.

II. Overview of 1ST and 2ND Order Discretization of Ordinary Differential Equations

In this section, we demonstrate the advantage of using second-order discretization methods over first-order methods by solving a 1st-order ordinary differential equation (ODE) given by Equation (1).

$$\dot{x}(t) = f(x(t),t) \tag{1}$$

The function f(x(t), t) is continuous and can be either linear or nonlinear. For linear functions with high order (greater than 2) or nonlinear functions, finding an analytical solution is either really difficult or impossible. Instead, an approximate solution is obtained by using numerical methods, which is based on replacing the first derivative by a discrete approximation using discretization methods. The discretization methods are classified as first-order methods, second-order methods, or higher-order methods. The most used first order discretization method is Forward Euler's method because of its simplicity, where $\dot{x}(t)$ is replaced by (2).

$$\dot{x}(t) = \frac{x(k\Delta t) - x((k-1)\Delta t)}{\Delta t} + O(\Delta t^2) \quad for\ (k-1)\Delta t \le t \le k\Delta t \tag{2}$$

This yields to the following discrete equation:

$$x_k = x_{k-1} + \Delta t f(x_k, t_k) \tag{3}$$

Where:

$$x_k = x(k\Delta t), \quad x_{k-1} = x((k-1)\Delta t),$$
$$t_k = k\Delta t, \quad f(x_k,t_k) = f(x(k\Delta t), k\Delta t).$$

Forward Euler's method is known to have a local truncation error of order O(Δt^2) and a global truncation error of order O(Δt), which is a disadvantage of this method. To obtain better results, we resort to improving the approximation by using second-order discretization schemes. The first second order method that we discuss is called central difference, which is based on approximating $\dot{x}(t)$ by (4).

$$\dot{x}(t) = \frac{x((k+1)\Delta t) - x((k-1)\Delta t)}{2\Delta t} + O(\Delta t^3) \quad for\ (k-1)\Delta t \le t \le (k+1)\Delta t \tag{4}$$

After replacing (4) in (1), we get the following multi step equation:

$$x_{k+1} = x_{k-1} + 2\Delta t f(x_k, t_k) \tag{5}$$

Central difference is known to have better accuracy than Forward Euler method in which the local error is of order O(Δt^3) instead of O(Δt^2), and the global error is of order O(Δt^2) instead of O(Δt). The Central Difference method is also known in the literature as the "Leap-Frog" method.

The Leap-Frog (Central Difference) method is better in terms of accuracy than Forward Euler. The method can also be easily implemented, requiring only one function evaluation per time step. However, its major disadvantage is that it has a risk of becoming unstable during long time integration. To handle this problem, the method is reinitialized using Forward Euler after each N steps of integration, ensuring the stability of the method [15].

Another method is the Adams-Bashforth scheme where the solution at time (k+1)Δt is expanded using Taylor's series formula:

$$x((k+1)\Delta t) \approx x(k\Delta t) + \Delta t\dot{x}(k\Delta t) + \frac{\Delta t^2}{2}\ddot{x}(k\Delta t) + O(\Delta t^3) \tag{6}$$

The second derivative is then approximated by Forward Euler's method:

$$\ddot{x}(k\Delta t) \approx \frac{\dot{x}(k\Delta t) - \dot{x}((k-1)\Delta t)}{\Delta t} \tag{7}$$

This yields to the following expression:

$$x_{k+1} \approx x_k + \frac{3\Delta t}{2} f(x_k,t_k) - \frac{\Delta t}{2} f(x_{k-1},t_{k-1}) + O(\Delta t^3) \quad for\ k\Delta t \le t \le (k+1)\Delta t \tag{8}$$

Adams-Bashforth method is also known to have better accuracy than Forward Euler method i.e, a local truncation error of order O(Δt^3) and a global truncation error of order O(Δt^2). The method can also be easily implemented, i.e. only a one function evaluation per step time is needed

In the rest of this section, a comparison between the methods stated above is illustrated by showing the solution obtained by each method and its error graphically. For this purpose, a simple ordinary differential equation is chosen, which is given by:

$$\dot{x}(t) = -x \tag{9}$$

With x(0) = 1.

Fig. 1 and 2 demonstrate the analytical response and the solutions obtained by the numerical methods stated above. The legend of Forward Euler is (FE), for the Leap-Frog (LP) and for Adams-Bashforth (AB2).

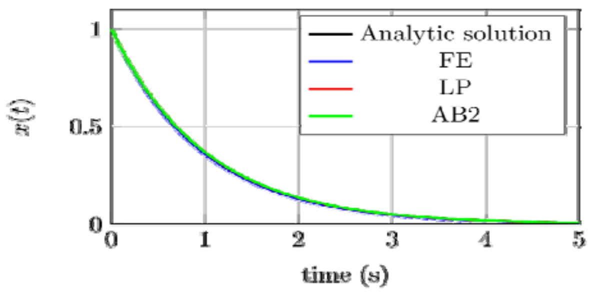

Fig.1. Comparison between Forward Euler, Leap-Frog, and AB2 methods response.

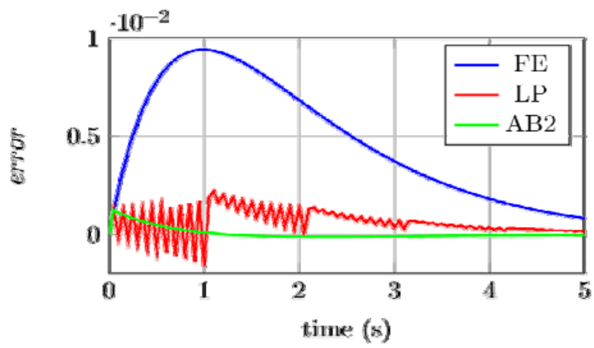

Fig.2. Errors of Forward Euler, Leap-Frog, and AB2solution with the analytical solution

We can see from Fig. 2 that the error of LP method is better than FE (almost one fifth the error of the Forward Euler's method) but it exhibits some oscillations; whereas AB2 method is the best in terms of accuracy and stability.

III. Dynamic Model of DFIG

Induction machines (IM) are very important in renewable energy domain. They are used extensively to generate electric power from wind energy. Different types of induction machine exist such as squirrel cage IM, permanent magnet IM…etc. However, Doubly-fed induction generators (DFIG) are best suited for wind turbines (WT) because they can produce a regulated electric power of constant voltage and frequency, regardless of the disturbance caused by the variation of wind speed. The ability to produce constant voltage and frequency electric power is ensured primarily by adjusting the amplitude and frequency of the voltage fed back to the rotor. Therefore, the output of the wind turbine that has a DFIG can be directly connected to the electric grid network [16-18]. A DFIG is composed of three-phase stator windings, which are the output of the machine, and a three-phase rotor winding, which is used as input to regulate the voltage and frequency of the three-phase stator voltage output. To derive a state space model of the DFIG, we express the voltage equations of both the stator and rotor referred to their natural reference frames. These equations are given by the references [19, 20].

(10) $$\begin{cases} v_{as} = R_s i_{as} + \dfrac{d\psi_{as}}{dt} \\ v_{bs} = R_s i_{bs} + \dfrac{d\psi_{bs}}{dt} \\ v_{cs} = R_s i_{cs} + \dfrac{d\psi_{cs}}{dt} \end{cases}$$ (11) $$\begin{cases} v_{ar} = R_r i_{ar} + \dfrac{d\psi_{ar}}{dt} \\ v_{br} = R_r i_{br} + \dfrac{d\psi_{br}}{dt} \\ v_{cr} = R_r i_{cr} + \dfrac{d\psi_{cr}}{dt} \end{cases}$$

Where $\psi_{as}, \psi_{bs}, \psi_{cs}$ are the three-phase stator fluxes,

and $\psi_{ar}, \psi_{br}, \psi_{cr}$ are the three-phase rotor fluxes.

To transform equations (10) and (11) to the (dq) rotating reference frame (Fig.3), we first need to transform them to the stationary two-phase components (αß) and then to the synchronous reference frame (dq). The resulting equation (12) is obtained as a result of this transformation process.

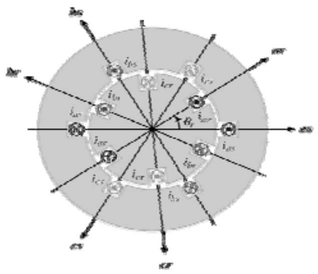

Fig.3. the (dq) reference frame of DFIG

(12) $$\begin{cases} v_{ds} = R_s i_{ds} + \dfrac{d\psi_{ds}}{dt} - \omega\psi_{qs} \\ v_{qs} = R_s i_{qs} + \dfrac{d\psi_{qs}}{dt} + \omega\psi_{ds} \\ v_{dr} = R_r i_{dr} + \dfrac{d\psi_{dr}}{dt} - (\omega - \omega_r)\psi_{qr} \\ v_{qr} = R_r i_{qr} + \dfrac{d\psi_{qr}}{dt} + (\omega - \omega_r)\psi_{dr} \end{cases}$$

Where:

(13) $$\begin{aligned} \psi_{ds} &= L_s i_{ds} + L_m i_{dr} \\ \psi_{qs} &= L_s i_{qs} + L_m i_{qr} \\ \psi_{dr} &= L_m i_{ds} + L_r i_{dr} \\ \psi_{qr} &= L_m i_{qs} + L_r i_{qr} \end{aligned}$$

With $\omega = \dfrac{d\theta}{dt}$ and $\omega_r = \dfrac{d\theta_r}{dt}$.

The mechanical torque of the DFIG machine is given by:

(14) $$T_m = T_{em} + J\frac{d\omega_r}{dt} + B\omega_r$$

The electromagnetic torque is then expressed in terms of stator current and rotor flux as:

(15) $$T_{em} = \frac{pL_m}{L_r}(\psi_{dr} i_{qs} - \psi_{qr} i_{ds})$$

By choosing a state vector $\underline{\mathbf{x}} = \begin{bmatrix} \psi_{dr} & \psi_{qr} & i_{ds} & i_{qs} & \omega_r \end{bmatrix}^T$, we obtain a state space model by combining equations (12-15), which is given by equation (16).

(16) $$\begin{pmatrix} \dot{\psi}_{dr} \\ \dot{\psi}_{qr} \\ \dot{i}_{ds} \\ \dot{i}_{qs} \\ \dot{\omega}_r \end{pmatrix} = \begin{bmatrix} -\dfrac{R_r}{L_r}\psi_{dr} + (\omega - \omega_r)\psi_{qr} + \dfrac{R_r L_m}{L_r} i_{ds} \\ -(\omega - \omega_r)\psi_{dr} - \dfrac{R_r}{L_r}\psi_{qr} + \dfrac{R_r L_m}{L_r} i_{qs} \\ \dfrac{R_r L_m}{\sigma L_r^2 L_s}\psi_{dr} - \dfrac{L_m}{\sigma L_s L_r}\omega_r\psi_{qr} - \dfrac{R_r L_m^2 + R_s L_r^2}{\sigma L_r^2 L_s} i_{ds} + \omega i_{qs} \\ \dfrac{L_m}{\sigma L_s L_r}\omega_r\psi_{dr} + \dfrac{R_s L_m}{\sigma L_r^2 L_s}\psi_{qr} - \omega i_{ds} - \dfrac{R_r L_m^2 + R_s L_r^2}{\sigma L_r^2 L_s} i_{qs} \\ \dfrac{pL_m}{JL_r}(\psi_{dr} i_{qs} - \psi_{qr} i_{ds}) - \dfrac{B}{J}\omega_r \end{bmatrix} + \begin{bmatrix} 1 & 0 & 0 & 0 & 0 \\ 0 & 1 & 0 & 0 & 0 \\ \dfrac{L_m}{\sigma L_s L_r} & 0 & \dfrac{1}{\sigma L_s} & 0 & 0 \\ 0 & \dfrac{L_m}{\sigma L_s L_r} & 0 & \dfrac{1}{\sigma L_s} & 0 \\ 0 & 0 & 0 & 0 & -\dfrac{1}{J} \end{bmatrix} \begin{pmatrix} v_{dr} \\ v_{qr} \\ v_{ds} \\ v_{qs} \\ T_m \end{pmatrix}$$

Equation (16) can be written in the form:

(17) $$\dot{\underline{\mathbf{x}}} = \mathbf{f}(\underline{\mathbf{x}}) + \mathbf{B}\underline{\mathbf{u}}$$

Where $\underline{\mathbf{u}} = \begin{bmatrix} v_{dr} & v_{qr} & v_{ds} & v_{qs} & T_m \end{bmatrix}^T$ and the output measurement vector is:

(18) $$\underline{\mathbf{z}} = \begin{bmatrix} i_{ds} & i_{qs} \end{bmatrix}^T = \mathbf{C}\underline{\mathbf{x}}$$

With $\mathbf{C} = \begin{bmatrix} 0 & 0 & 1 & 1 & 0 \end{bmatrix}$

The resulting state space model is nonlinear and will be used to estimate the speed and rotor flux of the DFIG machine.

IV. Extended Kalman Filter

The Kalman Filter (KF) is extensively used for state estimation in stochastic linear dynamical systems. The estimation is performed based on a recursive algorithm that estimates the state from prior knowledge given by the state space model and some measurements related to the estimated state. For nonlinear systems, the Kalman Filter can still be used for state estimation, but the nonlinear state space model has to be linearized before applying the algorithm. The resulting algorithm is known as the Extended Kalman Filter (EKF).

Whether for KF or EKF algorithm, the estimation process is done in two steps: a prediction step and a correction step. In the prediction step, we estimate the states by using the prior knowledge given by the state space model, and then we correct the estimation with the measurements performed and by calculating Kalman gain to get a better estimation. The Kalman gain is calculated by applying the minimum mean square error (MMSE) criteria to the state space model. The model is supposed to be not precise and is affected by random process noise vector w_{k-1} and the measurements are noisy and altered by a random noise vector v_k. Both w_{k-1} and v_k are assumed to be independent, have a Gaussian distribution of zero means and covariance matrices $\Sigma_{\tilde{w}}$ and $\Sigma_{\tilde{v}}$ respectively [21].

The DFIG state space model obtained in equation (16) has to be discretized in order to be used for state estimation by Kalman Filter algorithm [22].

The discretization of DFIG nonlinear model using Forward Euler's method gives the following discrete nonlinear model.

(19) $$\underline{\mathbf{x}}_k = \underline{\mathbf{x}}_{k-1} + \mathbf{\Delta t}\, \mathrm{f}(\underline{\mathbf{x}}_{k-1}) + \mathbf{B}_d \underline{\mathbf{u}}_{k-1}$$

Where: $\mathbf{B}_d = \mathbf{B}\Delta\mathbf{t}$, *Δt* – is the discretization step

The following steps summarizes the proposed EKF algorithm for DFIG machine:

Step 1: state-space discretization

$$\begin{cases} \mathbf{x}_k = \mathbf{x}_{k-1} + \Delta t f(\mathbf{x}_{k-1}) + \mathbf{B}_d \mathbf{u}_{k-1} + \mathbf{w}_{k-1} \\ \mathbf{z}_k = \mathbf{C}\mathbf{x}_k + \mathbf{v}_k \end{cases}$$

Step 2: Initialization

$$\hat{\mathbf{x}}_0^+ = E[\mathbf{x}_0]$$
$$\Sigma_{\tilde{x},0}^+ = E[(\mathbf{x}_0 - \hat{\mathbf{x}}_0^+)(\mathbf{x}_0 - \hat{\mathbf{x}}_0^+)^T]$$

Step 3: For $k = 1,2,...N$ **, calculate:**

Linearization:

$$\mathbf{A}_{k-1} = \frac{df(\mathbf{x}_{k-1})}{d\mathbf{x}_{k-1}}$$
$$\mathbf{A}_d = \mathbf{I} + \Delta t \mathbf{A}_{k-1}$$

Prediction:

$$\hat{\mathbf{x}}_k^- = \hat{\mathbf{x}}_{k-1}^+ + \Delta t f(\hat{\mathbf{x}}_{k-1}^+) + \mathbf{B}_d \mathbf{u}_{k-1} + \mathbf{w}_{k-1}$$
$$\Sigma_{\tilde{x},k}^- = \mathbf{A}_d \Sigma_{\tilde{x},k-1}^+ \mathbf{A}_d^T + \Sigma_{\tilde{w}}$$
$$\hat{\mathbf{z}}_k = \mathbf{C}\hat{\mathbf{x}}_k^- + \mathbf{v}_k$$

Correction:

$$\mathbf{L}_k = \Sigma_{\tilde{x},k}^- \mathbf{C}^T [\mathbf{C}\Sigma_{\tilde{x},k}^- \mathbf{C}^T + \Sigma_{\tilde{v}}]^{-1}$$
$$\hat{\mathbf{x}}_k^+ = \hat{\mathbf{x}}_k^- + \mathbf{L}_k(\mathbf{z} - \hat{\mathbf{z}}_k)$$
$$\Sigma_{\tilde{x},k}^+ = (\mathbf{I} - \mathbf{L}_k\mathbf{C})\Sigma_{\tilde{x},k}^-$$

Now, we develop the Extended Kalman Filter equations for the central difference method [23].

Step 1: The nonlinear discrete-time state-space representation:

$$\begin{cases} \mathbf{x}_k = \mathbf{x}_{k-2} + 2\Delta t f(\mathbf{x}_{k-1}) + 2\mathbf{B}_d \mathbf{u}_{k-1} + \mathbf{w}_{k-1} \\ \mathbf{z}_k = \mathbf{C}\mathbf{x}_k + \mathbf{v}_k \end{cases}$$

Step 2: Linearization of the equation yields to:

$$\mathbf{A}_{k-1} = \frac{df(\mathbf{x}_{k-1})}{d\mathbf{x}_{k-1}} \Rightarrow \mathbf{A}_d = 2\Delta t \mathbf{A}_{k-1}$$
$$\begin{cases} \mathbf{x}_k = \mathbf{x}_{k-2} + \mathbf{A}_d \mathbf{x}_{k-1} + 2\mathbf{B}_d \mathbf{u}_{k-1} + \mathbf{w}_{k-1} \\ \mathbf{z}_k = \mathbf{C}\mathbf{x}_k + \mathbf{v}_k \end{cases}$$

Step 3: The state prediction is:

$$\hat{\mathbf{x}}_k^- = \hat{\mathbf{x}}_{k-2}^+ + 2\Delta t f(\hat{\mathbf{x}}_{k-1}^+) + 2\mathbf{B}_d \mathbf{u}_{k-1}$$

The estimation error is:

$$\tilde{\mathbf{x}}_k^- = \mathbf{x}_k - \hat{\mathbf{x}}_k^- \approx \mathbf{A}_d \tilde{\mathbf{x}}_{k-1}^+ + \tilde{\mathbf{x}}_{k-2}^+ + \mathbf{w}_{k-1}$$

The error covariance matrix is obtained as follows:

$$\begin{aligned} \Sigma_{\tilde{x},k}^- &= \mathrm{E}[(\mathbf{x}_k - \hat{\mathbf{x}}_k^-)(\mathbf{x}_k - \hat{\mathbf{x}}_k^-)^T] \\ &= \mathrm{E}[(\mathbf{A}_d \tilde{\mathbf{x}}_{k-1}^+ + \tilde{\mathbf{x}}_{k-2}^+ + \mathbf{w}_{k-1})(\mathbf{A}_d \tilde{\mathbf{x}}_{k-1}^+ + \tilde{\mathbf{x}}_{k-2}^+ + \mathbf{w}_{k-1})^T] \\ &= E[\mathbf{A}_d \tilde{\mathbf{x}}_{k-1}^+ (\tilde{\mathbf{x}}_{k-1}^+)^T \mathbf{A}_d^T + \mathbf{A}_d \tilde{\mathbf{x}}_{k-1}^+ (\tilde{\mathbf{x}}_{k-2}^+)^T + \tilde{\mathbf{x}}_{k-2}^+ (\tilde{\mathbf{x}}_{k-1}^+)^T \mathbf{A}_d^T \\ &\quad + \tilde{\mathbf{x}}_{k-2}^+ (\tilde{\mathbf{x}}_{k-2}^+)^T + \mathbf{w}_{k-1}\mathbf{w}_{k-1}^T] \\ &= \mathbf{A}_d \Sigma_{\tilde{x},k-1}^+ \mathbf{A}_d^T + \mathbf{A}_d \Sigma_{\tilde{x}^+,(k-1,k-2)} + \Sigma_{\tilde{x}^+,(k-2,k-1)} \mathbf{A}_d^T \\ &\quad + \Sigma_{\tilde{x},k-2}^+ + \Sigma_w \end{aligned}$$

Where:

$$\begin{aligned} \Sigma_{\tilde{x}^+,(k-1,k-2)} &= E[\tilde{\mathbf{x}}_{k-1}^+ (\tilde{\mathbf{x}}_{k-2}^+)^T] \\ &= E[(\mathbf{A}_d \tilde{\mathbf{x}}_{k-2}^+ + \tilde{\mathbf{x}}_{k-3}^+ + \mathbf{w}_{k-2})(\tilde{\mathbf{x}}_{k-2}^+)^T] \\ &= \mathbf{A}_d \Sigma_{\tilde{x},k-2}^+ + \Sigma_{\tilde{x}^+,(k-3,k-2)} \end{aligned}$$

And:

$$\begin{aligned} \Sigma_{\tilde{x}^+,(k-2,k-1)} &= E[\tilde{\mathbf{x}}_{k-2}^+ (\tilde{\mathbf{x}}_{k-1}^+)^T] \\ &= E[\tilde{\mathbf{x}}_{k-2}^+ ((\mathbf{A}_d \tilde{\mathbf{x}}_{k-2}^+ + \tilde{\mathbf{x}}_{k-3}^+ + \mathbf{w}_{k-2}))^T] \\ &= \Sigma_{\tilde{x},k-2}^+ \mathbf{A}_d^T + \Sigma_{\tilde{x}^+,(k-2,k-3)} \end{aligned}$$

Compared to the classical EKF equations obtained by Forward Euler method, there are two new terms in these equations when using central difference discretization: $\Sigma_{\tilde{x}^+,(k-1,k-2)}$ and $\Sigma_{\tilde{x}^+,(k-2,k-1)}$. These terms are computed recursively as shown in the above equations.

As stated in section 2, central difference method suffers of instability problem for long-time integration, and the solution to this problem is to reinitialize the algorithm with Forward Euler after *N* steps [24, 25].

Lastly, we develop the extended Kalman filter for Adams-Bashforth 2nd order method:

Step 1: discrete-time state-space representation:

$$\begin{cases} \mathbf{x}_k = \mathbf{x}_{k-1} + \frac{3}{2}\Delta t f(\mathbf{x}_{k-1}) - \frac{1}{2}\Delta t f(\mathbf{x}_{k-2}) + \frac{\mathbf{B}\Delta t}{2}(3\mathbf{u}_{k-1} - \mathbf{u}_{k-2}) \\ \qquad + \mathbf{w}_{k-1} \\ \mathbf{z}_k = \mathbf{C}\mathbf{x}_k + \mathbf{v}_k \end{cases}$$

Step 2: Linearizing the equation yields to:

$$\mathbf{A}_{k-1} = \frac{df(\mathbf{x}_{k-1})}{d\mathbf{x}_{k-1}}, \quad \mathbf{A}_{k-2} = \frac{df(\mathbf{x}_{k-2})}{d\mathbf{x}_{k-2}}$$
$$\begin{cases} \mathbf{x}_k = \mathbf{A}_{d1}\mathbf{x}_{k-1} - \mathbf{A}_{d2}\mathbf{x}_{k-2} + \mathbf{B}_d(3\mathbf{u}_{k-1} - \mathbf{u}_{k-2}) + \mathbf{w}_{k-1} \\ \mathbf{z}_k = \mathbf{C}\mathbf{x}_k + \mathbf{v}_k \end{cases}$$

Where:

$$\mathbf{A}_{d1} = \mathbf{I} + \frac{3}{2}\Delta t \mathbf{A}_{k-1}, \ \mathbf{A}_{d2} = \frac{1}{2}\Delta t \mathbf{A}_{k-2}, \ \mathbf{B}_d = \frac{\mathbf{B}\Delta t}{2}$$

Step 3: The state prediction is:

$$\hat{\mathbf{x}}_k^- = \hat{\mathbf{x}}_{k-1}^+ + \frac{3}{2}\Delta t f(\hat{\mathbf{x}}_{k-1}^+) - \frac{1}{2}\Delta t f(\hat{\mathbf{x}}_{k-2}^+) + \mathbf{B}_d(3\mathbf{u}_{k-1} - \mathbf{u}_{k-2})$$

The estimation error is:

$$\tilde{\mathbf{x}}_k^- = \mathbf{x}_k - \hat{\mathbf{x}}_k^- \approx \mathbf{A}_d \tilde{\mathbf{x}}_{k-1}^+ + \mathbf{A}_{d2} \tilde{\mathbf{x}}_{k-2}^+ + \mathbf{w}_{k-1}$$

The error covariance matrix is obtained as follows:

$$\begin{aligned} \Sigma_{\tilde{x},k}^- &= E[(\mathbf{x}_k - \hat{\mathbf{x}}_k^-)(\mathbf{x}_k - \hat{\mathbf{x}}_k^-)^T] \\ &= E[(\mathbf{A}_{d1}\tilde{\mathbf{x}}_{k-1}^+ - \mathbf{A}_{d2}\tilde{\mathbf{x}}_{k-2}^+ + \mathbf{w}_{k-1})\ (\mathbf{A}_{d1}\tilde{\mathbf{x}}_{k-1}^+ - \mathbf{A}_{d2}\tilde{\mathbf{x}}_{k-2}^+ + \mathbf{w}_{k-1})^T] \\ &= E[\mathbf{A}_{d1}\tilde{\mathbf{x}}_{k-1}^+ (\tilde{\mathbf{x}}_{k-1}^+)^T \mathbf{A}_{d1}^T - \mathbf{A}_{d1}\tilde{\mathbf{x}}_{k-1}^+ (\tilde{\mathbf{x}}_{k-2}^+)^T \mathbf{A}_{d2}^T \\ &\quad - \mathbf{A}_{d2}\tilde{\mathbf{x}}_{k-2}^+ (\tilde{\mathbf{x}}_{k-1}^+)^T \mathbf{A}_{d1}^T + \mathbf{A}_{d2}\tilde{\mathbf{x}}_{k-2}^+ (\tilde{\mathbf{x}}_{k-2}^+)^T \mathbf{A}_{d2}^T + \mathbf{w}_{k-1}\mathbf{w}_{k-1}^T] \\ &= \mathbf{A}_{d1}\Sigma_{\tilde{x},k-1}^+ \mathbf{A}_{d1}^T - \mathbf{A}_{d1}\Sigma_{\tilde{x}^+,(k-1,k-2)}\mathbf{A}_{d2}^T - \mathbf{A}_{d2}\Sigma_{\tilde{x}^+,(k-2,k-1)}\mathbf{A}_{d1}^T \\ &\quad + \mathbf{A}_{d2}\Sigma_{\tilde{x},k-2}^+ \mathbf{A}_{d2}^T + \Sigma_w \end{aligned}$$

Where:

$$\Sigma_{\tilde{x}^+,(k-1,k-2)} = E[\tilde{\mathbf{x}}_{k-1}^+(\tilde{\mathbf{x}}_{k-2}^+)^T]$$
$$= E[(\mathbf{A}_{d1}\tilde{\mathbf{x}}_{k-2}^+ - \mathbf{A}_{d2}\tilde{\mathbf{x}}_{k-3}^+ + \mathbf{w}_{k-2})(\tilde{\mathbf{x}}_{k-2}^+)^T]$$
$$= \mathbf{A}_{d1}\Sigma_{\tilde{x},k-2}^+ - \mathbf{A}_{d2}\Sigma_{\tilde{x}^+,(k-3,k-2)}$$

And

$$\Sigma_{\tilde{x}^+,(k-2,k-1)} = E[\tilde{\mathbf{x}}_{k-2}^+(\tilde{\mathbf{x}}_{k-1}^+)^T]$$
$$= E[\tilde{\mathbf{x}}_{k-2}^+(\mathbf{A}_{d1}\tilde{\mathbf{x}}_{k-2}^+ - \mathbf{A}_{d2}\tilde{\mathbf{x}}_{k-3}^+ + \mathbf{w}_{k-2})^T]$$
$$= \Sigma_{\tilde{x},k-2}^+\mathbf{A}_{d1}^T - \Sigma_{\tilde{x}^+,(k-2,k-3)}\mathbf{A}_{d2}^T$$

As in the LP method, the new terms in these equations are: $\Sigma_{\tilde{x}^+,(k-1,k-2)}$ and $\Sigma_{\tilde{x}^+,(k-2,k-1)}$ which are computed recursively as shown in the equations above.

The following steps summarize the EKF algorithm for the Adams-Bashforth discretization applied for DFIG model [26].

Step 1: state-space discretization

$$\begin{cases} \mathbf{x}_k = \mathbf{x}_{k-1} + \Delta t f(\mathbf{x}_{k-1}) + \mathbf{B}_d\mathbf{u}_{k-1} + \mathbf{w}_{k-1} \\ \mathbf{z}_k = \mathbf{C}\mathbf{x}_k + \mathbf{v}_k \end{cases}$$

Step 2: Initialization

$$\hat{\mathbf{x}}_0^+ = E[\mathbf{x}_0]$$
$$\Sigma_{\tilde{x},0}^+ = E[(\mathbf{x}_0 - \hat{\mathbf{x}}_0^+)(\mathbf{x}_0 - \hat{\mathbf{x}}_0^+)^T]$$

Step 3: For $k = 1,2,...N$, calculate:

Linearization:

$$\mathbf{A}_{k-1} = \frac{df(\mathbf{x}_{k-1})}{d\mathbf{x}_{k-1}} \rightarrow \mathbf{A}_{d1} = \mathbf{I} + \frac{3}{2}\Delta t\mathbf{A}_{k-1}$$
$$\mathbf{A}_{k-2} = \frac{df(\mathbf{x}_{k-2})}{d\mathbf{x}_{k-2}} \rightarrow \mathbf{A}_{d2} = \frac{1}{2}\Delta t\mathbf{A}_{k-2}$$
$$\mathbf{B}_d = \frac{\mathbf{B}\Delta t}{2}$$

Prediction:

$$\hat{\mathbf{x}}_k^- = \hat{\mathbf{x}}_{k-1}^+ + \frac{3}{2}\Delta t f(\hat{\mathbf{x}}_{k-1}^+) - \frac{1}{2}\Delta t f(\hat{\mathbf{x}}_{k-2}^+) + \mathbf{B}_d(3\mathbf{u}_{k-1} - \mathbf{u}_{k-2})$$
$$\Sigma_{\tilde{x},k}^- = \mathbf{A}_{d1}\Sigma_{\tilde{x},k-1}^+\mathbf{A}_{d1}^T - \mathbf{A}_{d1}\Sigma_{\tilde{x}^+,(k-1,k-2)}\mathbf{A}_{d2}^T - \mathbf{A}_{d2}\Sigma_{\tilde{x}^+,(k-2,k-1)}\mathbf{A}_{d1}^T + \mathbf{A}_{d2}\Sigma_{\tilde{x},k-2}^+\mathbf{A}_{d2}^T + \Sigma_w$$
$$\hat{\mathbf{z}}_k = \mathbf{C}\hat{\mathbf{x}}_k^- + \mathbf{v}_k$$

Correction:

$$\mathbf{L}_k = \Sigma_{\tilde{x},k}^-\mathbf{C}^T[\mathbf{C}\Sigma_{\tilde{x},k}^-\mathbf{C}^T + \Sigma_{\tilde{v}}]^{-1}$$
$$\hat{\mathbf{x}}_k^+ = \hat{\mathbf{x}}_k^- + \mathbf{L}_k(\mathbf{z} - \hat{\mathbf{z}}_k)$$
$$\Sigma_{\tilde{x},k}^+ = (\mathbf{I} - \mathbf{L}_k\mathbf{C})\Sigma_{\tilde{x},k}^-$$

In the following section, the developed algorithms will be implemented to estimate the speed and rotor flux of a DFIG machine, then a comparison study will be discussed [27].

V. Results and Discussion

Table I. shows the DFIG rating parameters used for the simulation.

Table1. DFIG RATING PARAMETERS

Parameter	Rating values
Rated Power	3 kW
R_s	2.0 Ω
R_r	1.78 Ω
L_s	0.2406 H
L_r	0.2406 H
L_m	0.2304 H
Pole pairs	2
Moment of Inertia	0.0408 kg.m^2

Figure 4 shows the mechanical torque input used for simulation. We use variable mechanical torque, assuming it results from a variable wind speed hitting the wind turbine blades and rotating the DFIG rotor.

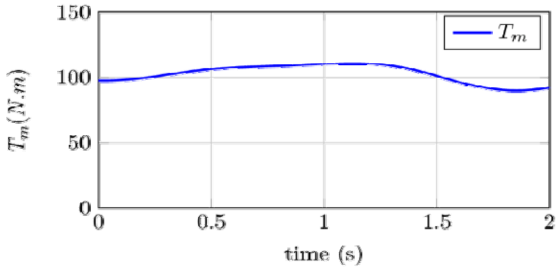

Fig.4. Input mechanical torque of the DFIG

For the purpose of simulation, the measured variables i_{ds} and i_{qs} are obtained from solving the DFIG equations numerically by using the *Runge-Kutta* algorithm. Then we add some measurement noise of covariance matrix:

$$\Sigma_{\tilde{v}} = \begin{bmatrix} \sigma_{v_1}^2 & 0 \\ 0 & \sigma_{v_2}^2 \end{bmatrix} = \begin{bmatrix} 10^{-1} & 0 \\ 0 & 10^{-1} \end{bmatrix} \quad (20)$$

Also, we need some process noise to the DFIG state space model with a covariance matrix given by:

$$\Sigma_{\tilde{w}} = \begin{bmatrix} 10^{-1} & 0 & 0 & 0 & 0 \\ 0 & 10^{-1} & 0 & 0 & 0 \\ 0 & 0 & 10^{-1} & 0 & 0 \\ 0 & 0 & 0 & 10^{-1} & 0 \\ 0 & 0 & 0 & 0 & 10^{-1} \end{bmatrix} \quad (21)$$

Figure 5 shows the stator currents of the DFIG machine. The current waveforms contain fluctuations resulting from the variation in mechanical torque applied to the DFIG machine [26, 27].

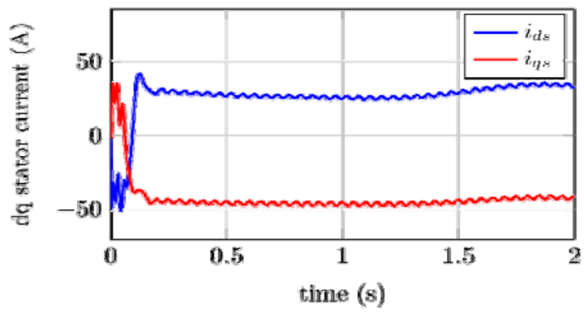

Fig.5. Stator and rotor currents

In what follows, the results of estimation using EKF corresponding to Forward Euler, central difference and Adams-Bashforth discretization methods will be discussed and compared. The estimated and simulated rotor speeds are shown in Fig. 6 where $\hat{\omega}_{r1}$ is for Forward Euler method, $\hat{\omega}_{r2}$ is for EKF with central Difference method and $\hat{\omega}_{r3}$ is for EKF with Adams-Bashforth method.

From Fig. 6, we can see that the rotor speed is better estimated with the Adams-Bashforth method than with the Forward Euler or Central Difference methods. Moreover, AB2 has better performance in both the transient regime and permanent response. This is due to the better accuracy of second-order methods over first-order methods. As shown in Fig. 6, the Central Difference discretization (LP method) results are noisy due to the instability problems discussed earlier. Overall, the AB2 with EKF gives better results with less noise in the response than LP with EKF or Forward Euler with EKF [29]. Table II gives the maximum errors of speed estimation for the three methods in both the transient regime and permanent regime.

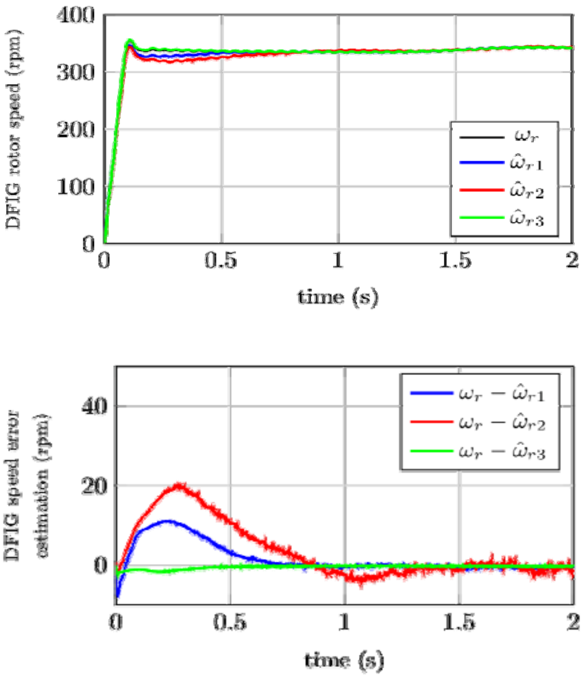

Fig.6. Rotor speed estimation of the DFIG

TABLE 2. MAX SPEED ERROR

Regime Response	FE-EKF Max. speed Error (RPM)	LP-EKF Max. speed Error (RPM)	AB2-EKF Max. speed Error (RPM)
Transient	10.99	19.89	2.70
Permanent	1.07	2.54	0.39

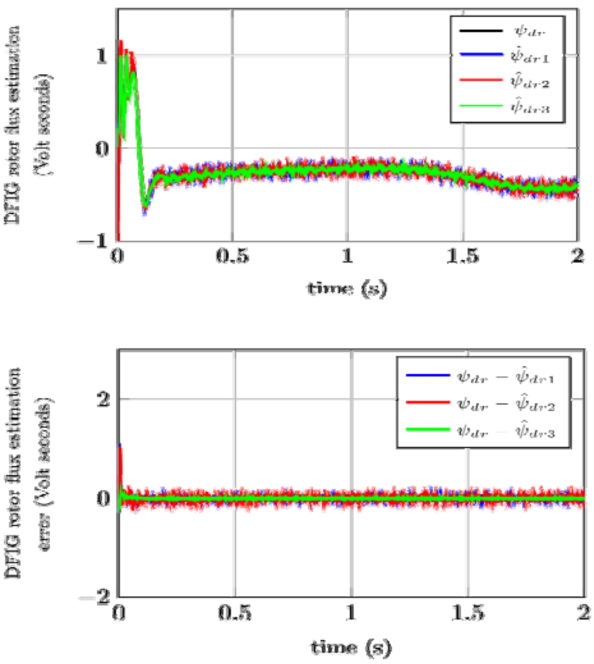

Fig.7. Estimated flux of DFIG rotor

Figures 7 and 8 demonstrate the estimated rotor flux by Forward Euler (FE), Leap-Frog (LP), and AB2 methods. The estimation of the rotor flux is better with AB2 than with FE and LP methods. As in speed estimation, the Central Difference discretization gives noisy estimation. The noisy response in the LP method is related to its instability problems over long-term integration. Similar to speed estimation, we can also say that AB2 with EKF is less noisy and more accurate than FE or LP with EKF. Overall, the rotor flux is better estimated with the AB2 method. Table III and Table IV give the maximum errors of flux estimation for the three methods in both transient and permanent regimes.

TABLE 3. MAX D-FLUX ERROR

Regime Response	FE-EKF Max. d-flux error (V.s)	LP-EKF Max. d-flux error (V.s)	AB2-EKF Max. d-flux error (V.s)
Transient	1.047	1.039	0.188
Permanent	0.056	0.113	0.017

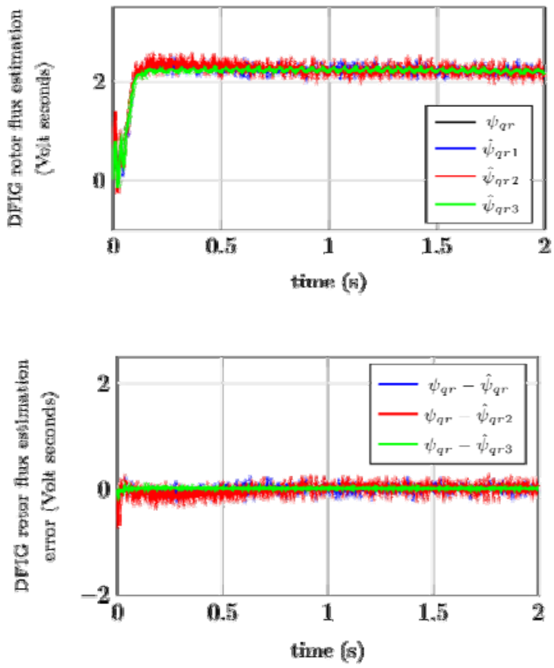

Fig. 8. q-component of DFIG rotor flux

TABLE 4. MAX Q-FLUX ERROR

Regime Response	FE-EKF Max. q-flux error (V.s)	LP-EKF Max. q-flux error (V.s)	AB2-EKF Max. q-flux error (V.s)
Transient	0.055	0.119	0.024
Permanent	0.381	0.693	0.102

VI. Conclusion

In this paper, a combination of second-order discretization methods with the Extended Kalman Filter (EKF) was proposed. Modified equations of the EKF have been introduced based on central difference and Adams-Bashforth discretization methods. The developed EKF algorithm is used to estimate the rotor speed and flux of a Doubly Fed Induction Generator (DFIG). From the obtained results, it was found that the EKF combined with Adams-Bashforth provides the best performance in terms of precision and stability. EKF with central difference has shown good performance, but the estimation results were a bit noisy due to instability problems, as discussed earlier. Based on these results, it is highly recommended to use the proposed EKF combined with Adams-Bashforth, as it provides the best accuracy with less complexity compared to other algorithms such as Unscented Kalman Filter (UKF) and Cubature Kalman Filter (CKF). For future work, it is highly recommendable to implement the proposed approach in a test bench of a DFIG machine.

ACKNOWLEDGEMENTS

This study has been sponsored by DGRSDT (Diréction Générale de la Recherche Scientifique et Développement Technologique) Algiers, Algeria.

Conflict of Interset

The authors declare that they have no conflicts of interest and we do not have any financial relationship with the organization that sponsored the research.

***Author**: PhD Student. Ahmad BOUSSOUFA, Applied Automation Laboratory, Faculty of Hydrocarbons, University of M'hamed Bougara of Boumerdes, 35000, Algeria, E-mail: a.boussoufa@univ-boumerdes.dz*

REFERENCES

[1] P. Hippe, "Regular design equations for the discrete reduced-order kalman filter," Archives of Control Sciences 22(2):175–189, 2012. DOI: 10.2478/v10170-011-0019-x
[2] Z. Lin, Q. Yang, Z. Guo, J. Li, "An improved autoregressive method with kalman filtering theory for vessel motion predication," International Journal of Intelligent Engineering and Systems 4(4):11–18, 2011.
[3] R. Riane, M. Kidouche, R. Illoul, M. Z. Doghmane, "Unknown resistive torque estimation of a rotary drilling system based on kalman filter," IETE Journal of Research pp. 1–12, 2020. https://doi.org/10.1080/03772063.2020.1724834
[4] Laamari, Yahia, et al. "Highly nonlinear systems estimation using extended and unscented kalman filters." PRZEGLĄD ELEKTROTECHNICZN journal, pp.111-115, 2021. doi:10.15199/48.2021.05.20
[5] J. Havlík, O. Straka, "Performance evaluation of iterated extended kalman filter with variable step-length," In Journal of Physics: Conference Series, vol. 659, p. 012022. IOP Publishing, 2015. DOI: 10.1088/1742-6596/659/1/012022
[6] M. Z. Doghmane, M. Kidouche, "Decentralized controller robustness improvement using longitudinal overlapping Decomposition-Application to web winding system," Elektronika ir Elektronika, vol. 24, pp. 10-18, 2018. DOI: https://doi.org/10.5755/j01.eie.24.5.21837
[7] B. D. Anderson, J. B. Moore, "Optimal filtering," Prentice-Hall Information and System Science Series, Prentice-Hall, INC., Englewood Cliffs, New Jersey 07632, 2012.
[8] M. Moujahid, H. Ben Azza, M. Jemli, M. Boussak, "Speed Estimation by Using EKF Techniques for Sensor-Less DTC of PMSM with Load Torque Observer," *International Review of Electrical Engineering 9*(2), 35-43 (2014).
[9] H. Dai, L. Zou, et al., "Two second-order nonlinear extended kalman particle filter algorithms," Open Journal of Statistics 5(04):254, 2015. DOI: 10.4236/ojs.2015.54027
[10] S. Udomsuk, K. Areerak, T. Areerak, Kongpan Arrerak, "Speed Estimation of Three-Phase Induction Motor Using Kalman Filter," *International Review of Electrical Engineering 16*(6), 15-27. DOI: https://doi.org/10.15866/iree.v13i4.13451
[11] D. Beckmann, M. Dagen, T. Ortmaier, "Symplectic discretization methods for parameter estimation of a nonlinear mechanical system using an extended Kalman filter," In International Conference on Informatics in Control, Automation and Robotics, vol. 2, pp. 327–334. SCITEPRESS, 2016. DOI: 10.5220/0005973503270334
[12] M. Kidouche, et al., "Combining second order central difference discretization with extended kalman filter for rotor speed and flux estimation of a doubly-fed induction generator," In 2018 International Conference on Communications and Electrical Engineering (ICCEE), pp. 1–6. IEEE, 2018. DOI: 10.1109/CCEE.2018.8634518
[13] K. Szabat, T. Orlowska-Kowalska, "Optimal design of the extended kalman filter for the two-mass system using genetic algorithm," Archives of Electrical Engineering 55(3-4):237–254, 2006.
[14] I. Arasaratnam, S. Haykin, "Cubature kalman filters," IEEE Transactions on automatic control 54(6):1254–1269, 2009. DOI: 10.1109/TAC.2009.2019800
[15] S. A. S. Ari Aluthge, R. Estep, "Filtered leapfrog time integration with enhanced stability properties," Journal of Applied Mathematics and Physics 4:1354–1370, 2016. DOI: 10.4236/jamp.2016.47145
[16] S. Muller, M. Deicke, R. W. De Doncker. Doubly fed induction generator systems for wind turbines. IEEE Industry applications magazine 8(3):26–33, 2002. DOI: 10.1109/2943.999610
[17] G. Abad, J. Lopez, M. Rodriguez, et al., "Doubly fed induction machine: modeling and control for wind energy generation," vol. 85. John Wiley & Sons, 2011.
[18] Akroum, H., Kidouche, M., Grouni, S., & Zelmat, M. (2010). A Perfectly Symmetrical Configuration in Dual-Bridge Inverter Topology for Maximum Mitigation of EMI, Common-Mode Voltages and Common-Mode Currents. *Elektronika Ir Elektrotechnika*, *103*(7), 51-56. https://eejournal.ktu.lt/index.php/elt/article/view/9275
[19] J. Slootweg, H. Polinder, W. L. Kling, "Dynamic modelling of a wind turbine with doubly fed induction generator," In 2001 Power Engineering Society Summer Meeting. Conference Proceedings (Cat. No. 01CH37262), vol. 1, pp. 644–649. IEEE, 2001. DOI: 10.1109/PESS.2001.970114
[20] A. Petersson, "Analysis, modeling and control of doubly-fed induction generators for wind turbines," PhD thesis, Chalmers University of Technology, 2005.
[21] D. Simon, "Optimal state estimation: Kalman, H infinity, and nonlinear approaches," John Wiley & Sons, 2006.
[22] Aibech, A., Akroum, H., Boudouda, A., Kidouche, M., & Doghmane, M. Z. (2021). Real-Time Reduction of Rotor Position Estimation Error Based on the Stator Flux Estimation-Combined Method for Sensorless Control of PMSMs Drives. *International Review of Electrical Engineering 16*(6), 15-27. DOI: https://doi.org/10.15866/iree.v16i6.20801
[23] M. Abdelrahem, C. Hackl, R. Kennel, "Application of extended kalman filter to parameter estimation of doubly fed induction generators in variable-speed wind turbine systems," In 2015 International Conference on Clean Electrical Power (ICCEP), pp. 226–233. IEEE, 2015. DOI: 10.1109/ICCEP.2015.7177628
[24] I. R. Pérez, J. C. Silva, E. J. Yuz, R. G. Carrasco, "Experimental sensorless vector control performance of a dfig based on an extended kalman filter," In IECON 2012-38th Annual Conference on IEEE Industrial Electronics Society, pp. 1786–1792. IEEE, 2012. DOI: 10.1109/IECON.2012.6388930
[25] M. K. Malakar, P. Tripathy, S. Krishnaswamy, "State estimation of dfig using an extended kalman filter with an augmented state model," In Power Systems Conference (NPSC), 2014 Eighteenth National, pp. 1–6. IEEE, 2014. DOI: 10.1109/NPSC.2014.7103891
[26] S. Yu, T. Fernando, H. H.-C. Iu, K. Emami, "Realization of state-
estimation-based dfig wind turbine control design in hybrid power systems using stochastic filtering approaches," IEEE Transactions on Industrial Informatics 12(3):1084–1092, 2016. DOI: 10.1109/TII.2016.2549940
[27] A. Boussoufa, M. Kidouche, A. Ahriche, "Rotor speed and flux estimation of a doubly-fed induction machine using extended kalman filter," Algerian Journal of Signals and Systems 2(4):266–273, 2017. DOI: https://doi.org/10.51485/ajss.v2i4.52
[28] D. J. Herzfeld, P. A. Vaswani, M. K. Marko, R. Shadmehr, "A memory of errors in sensorimotor learning," Science 345(6202):1349–1353, 2014. DOI: 10.1126/science.1253138
[29] Mendil C., Kidouche M., Doghmane M.Z. (2021) A Study of the Parametric Variations Influences on Stick-Slip Vibrations in Smart Rotary Drilling Systems. In: Hatti M. (eds) Artificial Intelligence and Renewables Towards an Energy Transition. ICAIRES 2020. Lecture Notes in Networks and Systems, vol 174. Springer, Cham. https://doi.org/10.1007/978-3-030-63846-7_67
[30] Mendil C., Kidouche M., Doghmane M.Z. (2021) Modeling of Hydrocarbons Rotary Drilling Systems Under Torsional Vibrations: A Survey. In: Hatti M. (eds) Artificial Intelligence and Renewables Towards an Energy Transition. ICAIRES 2020. Lecture Notes in Networks and Systems, vol 174. Springer, Cham. https://doi.org/10.1007/978-3-030-63846-7_24